

Patterning small-molecule biocapture surfaces: microcontact insertion printing vs. photolithography

M. J. Shuster,^{ab} A. Vaish,^{ab} H. H. Cao,^b A. I. Guttentag,^b J. E. McManigle,^a A. L. Gibb,^a
M. M. Martinez,^a R. M. Nezarati,^a J. M. Hinds,^a W.-S. Liao,^b P. S. Weiss^{*ab} and
A. M. Andrews^{*b}

^aCenter for Nanoscale Science, The Pennsylvania State University, University Park, PA 16802, USA

^bCalifornia NanoSystems Institute, UCLA, Los Angeles, CA 90095, USA. E-mail: aandrews@mednet.ucla.edu or psw@cnsi.ucla.edu

Online Supplemental Material

Materials and Methods

Chemicals: 23-(9-Mercaptononyl)-3,6,9,12,15,18,21-heptaoxatricosanoic acid (HEG) and 1-(9-mercaptononyl)-3,6,9-trioxaundecan-11-ol (TEG) were purchased from Toronto Research Chemicals (Toronto, ON, Canada). 1-(9-Mercaptononyl)-3,6,9,12,15,18-hexaoxaundecan-11-biotin (BEG) was purchased from ProChimia (Sopot, Poland). *N*-Hydroxysuccinimide (NHS), *N*-ethyl-*N*-(dimethylaminopropyl)-carbodiimide (EDC), 5-hydroxytryptamine hydrochloride (5-HT), 3,4-hydroxytyramine hydrochloride (3,4-dihydroxyphenylethylamine; dopamine; DA), and bovine serum albumin (BSA) were obtained from Sigma-Aldrich (St. Louis, MO, USA). Commercial grade ethanol (EtOH) was from Pharmaco-AAPER (Brookfield, CT, USA). Rabbit anti-serotonin polyclonal antibodies and rabbit anti-dopamine polyclonal antibodies were procured from Millipore (Temecula, CA, USA). AlexaFluor 488-labeled goat anti-rabbit antibodies (absorbance max at 495 nm, emission max at 519 nm), AlexaFluor 546-labeled goat anti-rabbit antibodies (absorbance max at 556 nm, emission max at 573 nm), streptavidin, and AlexaFluor 488-tagged streptavidin (absorbance max at 494 nm, emission max at 521 nm) were purchased from

Invitrogen (Carlsbad, CA, USA). Fluorescein isothiocyanate (FITC)-tagged anti-streptavidin polyclonal antibodies were purchased from Abcam (Cambridge, MA, USA).

Substrate formation: Metalized surfaces were fabricated by thermal evaporation of either 5 nm Cr and 15 nm Au on glass microscopy slides (photolithographic patterning) or 10 nm Cr and 100 nm Au on Si wafers (soft lithography patterning) (SiliconQuest, Santa Clara, CA, USA) using an electron beam evaporator (Kurt Lesker Inc., Clairton, PA, USA). Both metals were deposited at a rate of 1 Å/sec. Substrates were flame-annealed with a hydrogen flame immediately prior to monolayer formation.

Monolayer preparation: Self-assembled monolayers were prepared by exposing Au surfaces to a 1 mM solution of either TEG or HEG. After patterning by photolithography or μ CIP, surfaces with HEG were exposed to a solution of 15 mM NHS and 25 mM EDC for 1 h to create an activated ester bond between NHS and the carboxyl group of the HEG molecules on the surfaces. The NHS acts as a leaving group in the presence of the primary amine of 5-HT or DA, resulting in amide bond formation between 5-HT or DA and HEG and tethering of 5-HT or DA to surfaces only in regions containing carboxyl-terminated oligo(ethylene glycol) thiols.¹ Both 5-HT and DA solutions were prepared at 25 mM in phosphate-buffered saline (PBS). For 5-HT, PBS pH was 9.5, and samples were incubated at room temperature for 4 h. For DA, PBS pH was 6.75, and samples were incubated at 4 °C overnight. The lower temperature and pH for DA, which necessitates the longer incubation time, is required to reduce spontaneous oxidation in solution. In cases where BEG was used in place of HEG, the biotin epitope was attached to the thiol molecules by the manufacturer.

Photolithographic patterning: Photolithography on monolayers was accomplished using a bilayer resist stack and a series of pattern transfer techniques, as described elsewhere.² Briefly, a resist stack consisting of a non-photosensitive lift-off resist (LOR 5A, MicroChem Corp., Newton, MA) on the bottom and a photoresist (Shipley 3012, Shipley Company, Marlborough, MA) on the top was spin-coated on SAMs. Samples were then exposed to 365 nm light at a power of 12 mWcm⁻² using a contact aligner (MA-6, Karl Suss America, Inc., Waterbury Center, VT, USA), and patterns were transferred to the LOR during photoresist development. The photoresist was removed with an acetone rinse because of its instability under standard self-assembly conditions. The LOR then acted as a mask during UV-ozone exposure, which removed the SAMs in regions not protected by the LOR. A different thiol species (TEG or HEG) was then deposited on the newly exposed Au by immersing samples in a 1 mM thiol solution in EtOH, and the LOR was subsequently removed using a 2% tetramethyl ammonium hydroxide solution, leaving a patterned monolayer. A total of eight samples were prepared and analyzed using this technique, with five of the eight samples prepared with an initial TEG monolayer and three prepared with an initial HEG monolayer.

Stamp preparation: Polydimethylsiloxane (PDMS) stamps were prepared by mixing Dow Corning Sylgard 184 oligomer with the catalyst at a 10:1 ratio by weight. The mixture was then degassed, poured onto a silanized Si master wafer, and degassed again. This preparation was then baked at 75 °C for 24 h, after which the cured PDMS was removed from the wafer and cut into 1 cm × 2 cm squares. Stamps were cleaned by soaking in hexane for 1.5 h three times, followed by baking at 75 °C for 24 h to remove absorbed hexane.

Soft lithography by microcontact insertion printing: Immediately prior to use, stamps were sonicated in a 50/50 mixture EtOH and 18.2 MΩ deionized water for 30 min, then pressed onto a clean Si wafer to remove surface contaminants. Subsequently, stamps were exposed to an oxygen plasma for 12 s using a Harrick plasma cleaner (Ithaca, NY, USA) operated under low radio frequency power (6.8 W) to create an intermediate hydrophilic surface to facilitate ink transfer from stamps to substrates.³ A 3 mM solution of either HEG or BEG was pipetted onto the patterned side of the stamp and allowed to sit for 60 s. The stamp was then dried and placed into firm contact with a substrate on which a TEG monolayer had already been assembled. Stamps stayed in contact with SAMs for printing for 1 h. The HEG or BEG molecules insert into the monolayer only where the PDMS stamp makes direct contact with the surface, resulting in a low density of HEG or BEG molecules distributed in a pattern commensurate with the topography of the PDMS stamp. The stamp was subsequently removed, and samples were rinsed with EtOH and dried under a stream of N₂, resulting in patterned monolayers. Experiments with HEG and BEG samples were repeated 3-5 times.

Fluorescence microscopy: Patterned, chemically functionalized samples were exposed to solutions of primary antibodies that were specific for either 5-HT or DA epitopes or to streptavidin, which binds to biotin, followed by a rinse with deionized water. Surfaces were then exposed to solutions of fluorescently tagged antibodies with affinity for primary antibodies or streptavidin. In all cases, 1% (w/v) BSA was added to solutions to minimize nonspecific binding. Both fluorescently labeled and unlabeled streptavidin were used for biocapture experiments. In experiments shown in Fig. 3, AlexaFluor 488-labeled streptavidin was used to simplify the incubation process and to rule out antibody cross reactivity.

Samples were examined using an inverted Nikon TE300 optical microscope (Melville, NY, USA) with a 40× objective and a xenon arc lamp light source. Filter cubes

appropriate for the different fluorophores were used for fluorescence imaging. Photolithographically assisted chemical patterning samples, which were prepared on transparent thin gold on glass substrates, were also imaged using transmitted visible light.

Nonspecific binding analysis: Nonspecific binding patterns were difficult to observe on control samples, *i.e.*, samples where primary antibodies were omitted. We used the statistical toolbox of Matlab (MathWorks, Natick, MA, USA) to perform principal component analysis (PCA) on fluorescence intensity data to gain information about the magnitude of nonspecific binding compared to specific binding. Principal component analysis provides a method for deconstructing a data set into an orthogonal set of basis vectors (principal components, PCs) ordered by the contribution of each PC to the variance of the data. To accomplish this for analysis of an image, a matrix is created in which the position of the pixel intensity data in the matrix is spatially correlated to the pixel location in the image. Using this matrix as a data set, the mean of each column of the matrix is subtracted from each entry in that column to adjust the column data mean to zero. The covariance matrix is then calculated and its eigenvectors determined. The square root of the eigenvalue associated with each eigenvector is proportional to the variance correlated with that eigenvector. To determine how many PCs are necessary to account for a chosen percentage of the variance, a cumulative sum of the eigenvalues, arranged from greatest to least, divided by the sum of all eigenvalues, is performed. The number of eigenvalues necessary to reach a desired threshold indicates the necessary number of PCs. We used a 90% threshold for the analysis presented below. Because PCA has no free parameters, it provides an objective method to assess correlations in a data set. In the case of image analysis and images with high contrast, patterns require only a small number of PCs to account for the majority (60% to 90%) of the variance in the pixel intensities of the images. Conversely, low-

contrast patterns or images without a clear pattern require a substantially greater number of PCs to reach the same variance threshold.

Analysis of 21 images of samples prepared using μ CIP indicates that over 90% of the variance of well-defined, relatively uniform patterns, such as those seen in Figs. 2D and 2E in the main text, can be explained using less than 1% of the PCs (10 PCs in a 1024×1024 pixel image). By contrast, for control samples with low nonspecific binding, where patterns were faint or not discernable, upwards of 10% of all principal components were needed to reach a 90% variance threshold.

Although this analysis does not allow determination of nonspecific binding levels *per se*, it provides a method for comparing specific *vs* nonspecific binding. Patterns that do not meet the 1% PC criteria for reaching a 90% variance threshold can be regarded as spurious, *i.e.*, low specific binding. Moreover, control sample images that do not require greater than 10% of PCs to reach a 90% variance threshold indicate failure of the control experiment, *i.e.*, high nonspecific binding.

Results

Limitations of photolithographically patterned small-molecule capture surfaces: Although photolithographically assisted chemical patterning is capable of creating spatially separated regions of different functional molecules, specific capture of high-affinity binding partners by surface-tethered small-molecule probes was difficult to accomplish. High-density regions of small-molecule-functionalized probes were associated with high levels of nonspecific adsorption of antibodies (Fig. S1A). Even without functionalization, high-density regions of HEG exhibit nonspecific binding of antibodies (Fig. S1B). To overcome this, low-density small-molecule-functionalized regions were created using insertion-directed self-assembly.

However, disruption of the protein-resistant properties of TEG regions by residual LOR resulted in fluorescent patterns with a reversal of the expected contrast (Fig. S1C).

Conclusions

While the biotin-streptavidin complex is an excellent test system, binding affinity is on the order of 10^{-14} M, making it amongst the highest affinity interactions found in nature and thus, not wholly representative of common biological interactions. In contrast, neurotransmitters have affinities, when tethered to surfaces, for their cognate antibodies on the order of 10^{-9} M.⁴ The ability to capture binding partners selectively with binding affinities in the nanomolar range suggests that μ CIP will be useful for many applications of biological interest.

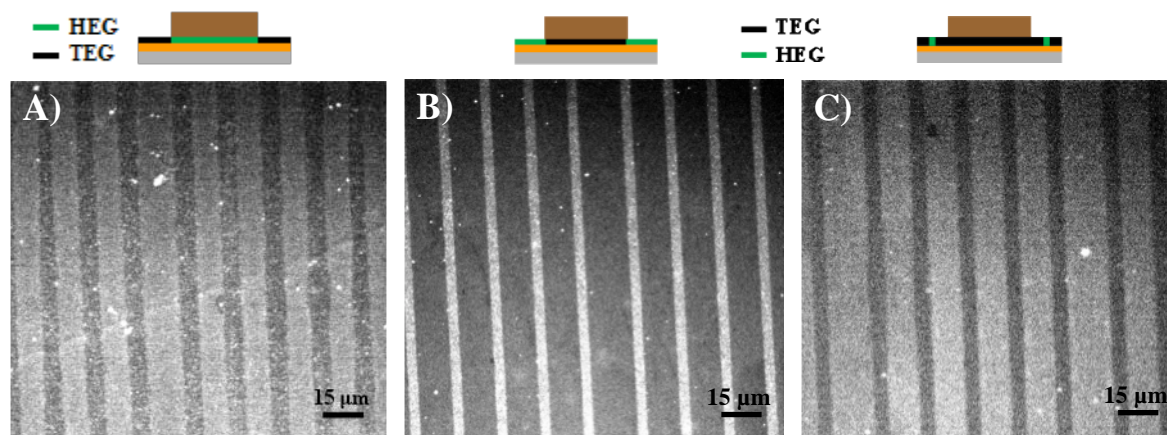


Figure S1: Limitations of photolithographically patterned small-molecule capture surfaces. **A)** Samples were prepared by creating densely packed SAMs of HEG followed by backfilling in unprotected regions with protein-resistant TEG. Regions containing HEG were functionalized with serotonin. These surfaces captured fluorescently tagged secondary antibodies in the serotonin functionalized HEG regions in the absence of primary anti-serotonin antibodies, indicating high nonspecific binding in the densely functionalized regions. **B)** Self-assembled monolayers of TEG were formed first, and HEG was backfilled in the photolithographically exposed regions. In this case, HEG was left unfunctionalized. Fluorescently tagged secondary antibodies showed recognition of densely packed regions of HEG in the absence of serotonin functionalization and primary anti-serotonin antibodies, indicating a high degree of nonspecific binding. **C)** Samples were prepared by forming monolayers of TEG followed by insertion of HEG into the unprotected regions, rather than backfilling. These samples showed an inverted contrast pattern such that TEG regions were brighter than serotonin-functionalized HEG regions after exposing surfaces to anti-serotonin primary antibodies and fluorescently tagged secondary antibodies. We hypothesize this type of pattern is due to residual LOR remaining in the protected TEG regions resulting in high nonspecific binding, which is greater than specific binding in the HEG inserted regions. For all images, wider stripes are the regions initially protected by the LOR.

References

1. M. J. Shuster, A. Vaish, M. E. Szapacs, M. E. Anderson, P. S. Weiss and A. M. Andrews, *Adv. Mater.*, 2008, **20**, 164.
2. M. E. Anderson, C. Srinivasan, J. N. Hohman, E. M. Carter, M. W. Horn and P. S. Weiss, *Adv. Mater.*, 2006, **18**, 3258.
3. A. Vaish, M. J. Shuster, S. Cheunkar, P. S. Weiss and A. M. Andrews, *Small*, 2011, **7**, 1471.
4. T. Wang and J. Muthuswamy, *Anal. Chem.*, 2008, **80**, 8576.